Chapter 2
Aerosol Mass Transfer

The size distribution of aerosol particles has a significant impact on their chemical and physical properties, including their optical properties and ability to act as cloud condensation nuclei in the atmosphere [1]. Understanding the factors which determine the particle size underpins all of aerosol science and is essential for the construction of accurate atmospheric models of past, present and future climate [2].

This chapter will outline the thermodynamic and kinetic factors which control the size of aerosol particles, in particular aqueous aerosol droplets containing inorganic and organic solutes. Theory predicting thermodynamic equilibrium droplet size will first be discussed, followed by a description of the kinetic aspects of aerosol mass transfer which can limit the rate at which the equilibrium size is established.

2.1 Thermodynamic Equilibrium Droplet Size

Water plays a highly significant role in the atmosphere as a result of its abundance and is the major constituent of clouds. Atmospheric water exists in the gas-phase and in the condensed phase as aerosol droplets and ice particles. Aqueous aerosol droplets will rarely consist of pure water; instead they will contain a range of soluble and insoluble species depending on where and how they formed. The discussion here will therefore focus on the equilibrium size of aqueous droplets containing common atmospheric constituents such as inorganic salts.

2.1.1 Deliquescence and Efflorescence

The size of aqueous aerosol droplets is determined by the equilibrium partitioning of water into the condensed phase and, thus the relative humidity of the droplet

K. J. Knox, *Light-Induced Processes in Optically-Tweezed Aerosol Droplets*,
Springer Theses, DOI: 10.1007/978-3-642-16348-7_2,

environment. This relative humidity, RH, is defined as the ratio of the partial pressure of water, p_w, to the temperature-dependent saturation vapour pressure of water, $p^0_{,}$ and is often expressed as a percentage, hence [1]:

$$\mathrm{RH} = \frac{p_w}{p^0} \times 100 \tag{2.1}$$

Inorganic salt particles are solid and crystalline at low RH, while at higher RH they take up water and become solution droplets. The variation of particle water content does not vary smoothly with RH over the entire range from 0 to 100%. A solid particle of an inorganic salt does not take up water significantly until a critical RH is reached, known as the deliquescence RH (DRH), which is characteristic of the salt in question. At this RH a phase transition occurs and the particle abruptly takes up water, producing a saturated salt solution. As the RH increases further the particle grows by absorbing more water. If the RH decreases the particle will lose water by evaporation until the particle crystallises at a characteristic RH. This crystallisation RH (CRH) is not found to be equal to the DRH. In fact the CRH is generally considerably lower than the DRH. As a result there is a range of RH, between the CRH and DRH, over which an aerosol droplet can exist in a supersaturated metastable state. This metastable state exists because nucleation sites are required for crystallisation of the salt content of the droplets. In free aerosol particles these are not available and a droplet must first reach a state of critical supersaturation before nucleation and crystallisation can take place. This hysteresis is illustrated in Fig. 2.1 for NaCl, calculated using the Aerosol Inorganics Model (AIM), which was developed by Clegg et al. in 1998 [3]. The variation of the total particle mass with RH is expressed relative to the dry particle mass. It should be noted that some compounds, for example H_2SO_4 and some organic compounds, take up or lose water smoothly as the RH is increased or decreased, respectively. This is a result of their highly hygroscopic nature. The behaviour of H_2SO_4 is also shown in Fig. 2.1.

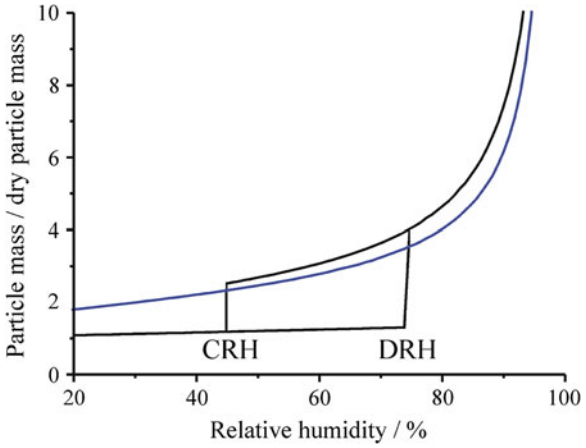

Fig. 2.1 Variation in particle mass, relative to the dry particle mass, with RH at 25 °C for NaCl and H_2SO_4, shown in *black* and *blue*, respectively. Calculated using AIM [3]

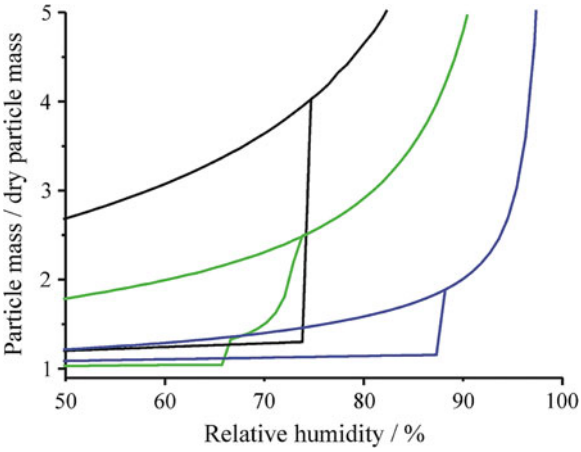

Fig. 2.2 Deliquescence behaviour of an NaCl, glutaric acid and mixed composition particle consisting of NaCl and glutaric acid (57 and 43% by mass, respectively) at 25°C, shown in *black*, *blue* and *green* respectively. Calculated using AIM [3]

Most aerosol mass is in fact of mixed composition. In this situation similar behaviour is observed, however, 'stepped' deliquescence occurs over an RH range determined by the mixture of the species in the droplet [4]. An example is provided in Fig. 2.2 for a mixture of NaCl (57% by mass) and glutaric acid (43% by mass), again calculated using AIM. The variation of particle mass with RH for NaCl and glutaric acid particles is included for comparison; it can be seen that deliquescence for the mixed composition particle occurs at a lower RH than the DRH of both pure NaCl and glutaric acid particles and is not abrupt.

The inorganic salt used in most of the experiments discussed in this thesis is NaCl, which has a DRH of 75.3 ± 0.1 [4]. The experiments are performed under conditions of high RH of ~85–98%; they are therefore not complicated by crystallisation and the droplet size can be considered to vary smoothly with RH.

2.1.2 Variation of Droplet Size with Relative Humidity above the DRH

The factors determining the equilibrium size of an aqueous droplet can be understood by considering the partial pressure of water at the droplet surface with variation in solute concentration or, equivalently, droplet size. A droplet will be at equilibrium if the partial pressure of water at its surface, $p_{w,d}$, is equal to that in the surrounding gas-phase, p_w. The p_w is determined by the RH. The factors determining $p_{w,d}$ are the curvature of the droplet surface and the droplet solute concentration.

The curvature or Kelvin effect describes the observation that the vapour pressure of a substance above a curved surface is greater than that above a flat surface. For a pure water droplet, the smaller the radius the higher the degree of curvature

and hence the higher the vapour pressure above the droplet surface. This effect arises because a molecule at a curved interface has fewer neighbouring molecules than one at a flat interface, and hence the sum of the intermolecular forces experienced by the molecule is lower. As a result less energy is required to liberate such a molecule into the gas phase. The effect is described by Kelvin equation [1]:

$$\frac{p_c}{p^0} = \exp\left(\frac{2M_w\sigma_w}{RT\rho_w r}\right) \tag{2.2}$$

where p_c is the vapour pressure above a curved water droplet surface, M_w is the molar weight of water, σ_w is the surface tension of a water/air interface, R is the molar gas constant, T is the temperature, ρ_w is the density of water and r is the droplet radius. A consequence of this effect is that a pure water droplet would require an RH of $> 100\%$ in its surroundings to maintain a stable equilibrium size. The effect of curvature on the p_c is only significant for droplet radii of less than ~ 0.05 μm, as illustrated by Fig. 2.3.

The solute effect describes the observation that the addition of a solute to a solution reduces the vapour pressure of the solvent at the surface. In an ideal solution the added solute molecules take the place of some of the solvent molecules in the solution and this reduces the mole fraction and thus the vapour pressure of the solvent at the interface. Hence the solute effect is given by Raoult's law [1]:

$$p_{w,s} = x_w p^0 \tag{2.3}$$

where $p_{w,s}$ is the vapour pressure of water above a solution and x_w is the mole fraction of water in the droplet. For a droplet containing a fixed amount of solute, as the droplet radius increases the solute will become more dilute, diminishing the solute effect.

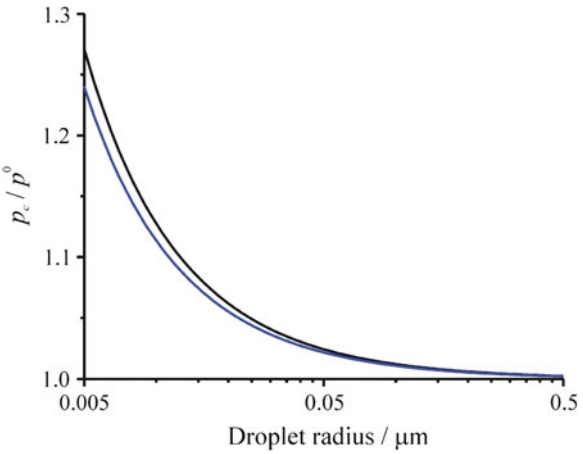

Fig. 2.3 The variation of the ratio of the vapour pressure of water over a droplet to that over a flat surface with droplet diameter at 273 and 293 K, shown in *black* and *blue*, respectively

For non-ideal solutions solute–solvent interactions must be considered. These are accounted for by replacing x_w with the activity of water, a_w, which is defined by

$$a_w = \gamma_w x_w \tag{2.4}$$

where γ_w is the concentration-dependent activity coefficient of water. The solute effect is therefore described by [1]

$$p_{w,s} = a_w p^0 \tag{2.5}$$

Determining γ_w for combinations of solutes at varying concentrations is a key challenge in gaining an understanding of the thermodynamic behaviour of aqueous atmospheric aerosols [5]. For dilute solutions $\gamma_w \rightarrow 1$ and the solution behaviour can be considered ideal.

The combination of these two factors determines the vapour pressure at the surface of a droplet containing a solute and thus the droplet size which is in equilibrium with a given surrounding gas-phase partial pressure of water [1]:

$$\frac{p_{w,d}}{p^0} = a_w \exp\left(\frac{2M_w\sigma_w}{RT\rho_w r}\right) \tag{2.6}$$

In the limit of dilute solutions this expression can be expressed in a simplified form [1]:

$$\ln\left(\frac{p_{w,d}}{p^0}\right) = \frac{2M_w\sigma_w}{RT\rho_w r} - \frac{3n_s M_w}{4\pi\rho_w r^3} \tag{2.7}$$

where n_s is the number of moles of solute in the droplet; the solute is assumed to be non-volatile and hence n_s will remain constant as the droplet size changes.

This approach to understanding equilibrium droplet size was first proposed by Köhler in 1921 [6]. Figure 2.4 shows the equilibrium behaviour of aqueous NaCl

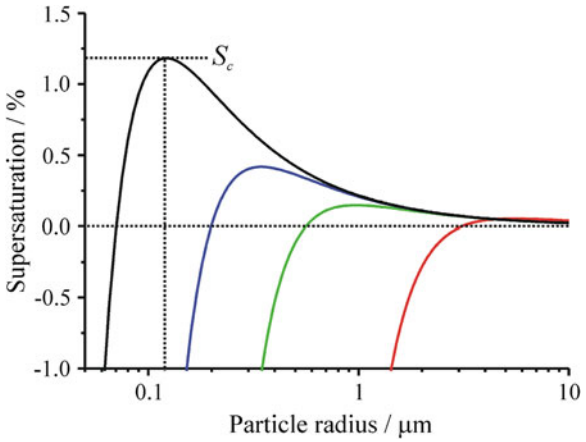

Fig. 2.4 Köhler curves for NaCl particles with $r_d = 0.01$, 0.02, 0.04 and 0.08 μm shown in *black*, *blue*, *green* and *red* respectively. S_c labels the critical supersaturation for the droplet with the smallest dry particle radius

aerosol droplets of various dry particle radii, r_d, with varying supersaturation, S, which is the RH expressed relative to 100%, calculated using Eq. 2.7 introduced above. The dry particle radius is calculated from the droplet solute mass loading and the density of the solute, assuming a spherical geometry. It can be seen from Fig. 2.4 that particles with a larger solute loading, and hence r_d, attain a larger equilibrium size at a given RH.

These 'Köhler curves' are determined by both the solute and curvature effects. At subsaturations or for large r_d the solute effect determines the form of the curve and in order to maintain $p_{w,d}$ equal to p_w the droplet size increases with increasing RH. As the droplet size increases and the solute becomes more dilute the Kelvin effect becomes relatively more important. As a result there is a critical size above which a droplet will spontaneously take up water, limited only by the kinetics of mass transfer. The supersaturation corresponding to the critical size is termed the critical supersaturation, S_c, and is labelled for the droplet with the smallest dry particle radius in Fig. 2.4. Aerosol particles can act as cloud condensation nuclei in the atmosphere and are considered 'activated' once they have surpassed the transition to this regime of spontaneous growth, within which they will go on to become cloud droplets. The activation of aerosol particles is a process of critical importance as a result of the significance of clouds in determining the radiative balance of the atmosphere [1].[1]

The droplets relevant to the experiments presented in this thesis are of diameters of $\sim$6–16 μm, and as a result it is not necessary to include the Kelvin effect when considering equilibrium droplet behaviour under these conditions [1]. The droplet size can therefore be predicted from:

$$\frac{p_{w,d}}{p^0} = a_w \tag{2.8}$$

As mentioned earlier, determining the variation of a_w with solute concentration is not trivial. In these studies the following empirical relationship is used to relate the particle size to r_d and the RH [5, 7]:

$$\mathrm{GF} = \left[1 + \left(a + bRH + cRH^2\right)\frac{RH}{1 - RH}\right]^{\frac{1}{3}} \tag{2.9}$$

where GF is the droplet growth factor, which is defined as the ratio of the particle radius, also termed the wet particle radius, r_w, to r_d:

$$\mathrm{GF} = \frac{r_w}{r_d} \tag{2.10}$$

and a, b and c are experimentally-determined constants which are specific to the solute present in the aqueous droplet.

[1] See Sect. 1.1.2 for a detailed discussion.

In several experiments mixed composition droplets are investigated. In order to predict the equilibrium behaviour of such droplets the Zdanovskii, Stokes and Robinson (ZSR) approximation is used, which assumes that each component takes up water independently [5]. For example, for a droplet composed of two or more solutes the mass loading of each solute would be determined, and from these the volume of water which would be associated with each component would be calculated by using Eq. 2.9 and the appropriate values of a, b and c. A volume sum would then be used to determine the overall r_w of the mixed composition droplet.

2.2 Kinetics of Aerosol Mass Transfer

Understanding the kinetics of mass transfer between the gaseous and condensed phases of aerosols is of crucial importance for rationalising many atmospheric processes, for example heterogeneous chemistry at the surface of aerosol particles and the formation and stability of clouds [1, 8–11]. Although the equilibrium state can be readily predicted, it is often important to consider if the aerosol size distribution can legitimately be considered to be determined solely by thermodynamic principles. Two key quantities central to aerosol mass transfer are the mass accommodation coefficient, α, and the evaporation coefficient, γ_e. These quantities play a role in determining the rate of uptake of gaseous species by, and evaporation from, aerosol particles, respectively, governing the timescale for a droplet to attain a thermodynamic equilibrium size.

In the work presented in Chap. 7 a new technique for the determination of α and γ_e for the uptake or evaporation of water at an aqueous surface is demonstrated. These quantities have been the subject of many experimental studies, yet remain the subject of much debate [9, 12]. As well as studying the mass transfer of water to and from aqueous droplets containing only inorganic solutes, the effect of dissolved organic compounds on mass transfer is also investigated. The process of uptake of water at an aqueous surface and its atmospheric importance will now be discussed in detail, followed by a description of the differences and similarities in the case of evaporation.

2.2.1 Uptake by a Liquid Aerosol Droplet

The incorporation of a gaseous species into a liquid aerosol droplet can involve the combination of a number processes, as illustrated in Fig. 2.5 [12]. First, the molecule must diffuse in the gas phase to the region close to the droplet surface. It must then be accommodated at the particle surface and transferred to the bulk. Surface-adsorbed molecules may desorb back into the gas phase. Surface and liquid-phase reactions may occur, and surface and liquid-phase diffusion may play a role in determining the uptake rate.

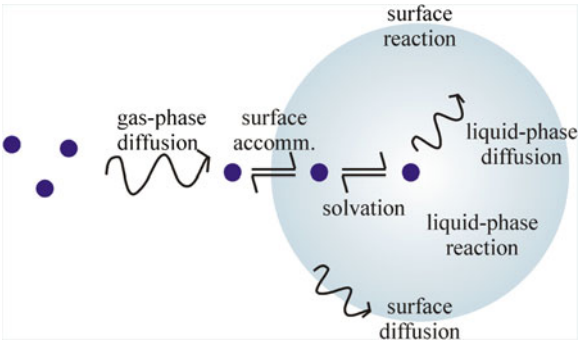

Fig. 2.5 Range of processes involved in uptake of a gas-phase species by a liquid aerosol particle

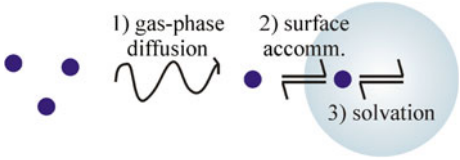

Fig. 2.6 Illustration of uptake as a three-step process

For non-reactive uptake of water into an aqueous droplet, which is considered in this work, the picture is simplified, as shown in Fig. 2.6.

The maximum possible rate of uptake, $J_{u,max}$ (molecules m^{-2} s^{-1}), is given by the collision rate of gas-phase molecules with a surface, which is defined by the Hertz–Knudsen equation [12, 13]:

$$J_{u,\max} = \frac{\Delta p_v}{\sqrt{2\pi M_a k_B T}} \tag{2.11}$$

where Δp_v is the water vapour pressure difference between the surrounding environment and the particle surface (Pa), M_a is the relative molecular mass of the adsorbing species (kg), k_B is the Boltzmann constant (J K^{-1}) and T is the temperature (K). This expression for J_u can be simplified using the mean speed of molecules in a gas, $\bar{c}$ (m s^{-1}) [14]:

$$\bar{c} = \sqrt{\frac{8k_B T}{\pi M_a}} \tag{2.12}$$

and the ideal gas law to express Δp_v as the corresponding difference in molecular density of gas molecules, Δn_g (molecules m^{-3}) The resulting simplified expression for $J_{u,max}$ is [12]:

$$J_{u,\max} = \frac{\Delta n_g \bar{c}}{4} \tag{2.13}$$

While this represents the maximum possible rate, there are several kinetic factors which will limit the actual rate of uptake observed. For non-reactive uptake these factors can be related to the three-steps shown in Fig. 2.6.

(1) Diffusion: As the gas-phase molecules of interest enter the surface their concentration is depleted near to the surface and more must travel to the region close to the surface by gas-phase diffusion. Unless diffusion is fast enough the collision rate, and thus flux, is diminished.
(2) Surface accommodation: The proportion of colliding molecules which become incorporated into the particle must be considered. If less than 100% of the molecular collisions lead to incorporation then the mass flux will be diminished.
(3) Solvation: The relative rates of solvation and re-evaporation of the gaseous molecules must be considered.

The combined effect of these factors on the rate of uptake can be expressed by a measured uptake coefficient, γ_{meas}. The measured rate of uptake, J_{meas}, will thus be given by the maximum rate of uptake multiplied by γ_{meas}, where $0 \leq \gamma_{meas} \leq 1$ [12]:

$$J_{meas} = \gamma_{meas} J_{u,\max} \tag{2.14}$$

2.2.1.1 The Resistance Model for Uptake

The individual contributions of the factors affecting γ_{meas} represent coupled differential equations which cannot be solved analytically [15]. The factors can, however, be conveniently considered using the resistance model of gas uptake, an approach first proposed by Schwartz [16, 17]. It assumes that the factors can be decoupled and so allows the effects to be examined separately. The approach is widely used [12, 15, 18, 19] and has been shown to introduce an error of $< 10\%$ compared with numerical solutions of the coupled problem [20, 21]. Using the resistance model gives the following expression describing the effect of the combined resistances in the case of non-reactive uptake [12, 15, 18, 19]:

$$\frac{1}{\gamma_{meas}} = \frac{1}{\Gamma_{diff}} + \frac{1}{\alpha} + \frac{1}{\Gamma_{sol}} \tag{2.15}$$

where $1/\Gamma_{diff}$ is used to describe the resistance to uptake as a result of the rate of gas-phase diffusion, α is the mass accommodation coefficient and $1/\Gamma_{sol}$ describes the resistance to uptake as a result of gas/liquid partitioning. The resistance model for gas uptake is analogous to that of electrical resistance in an electrical circuit. Figure 2.7 shows an electrical circuit analogy for non-reactive uptake. Continuing the electrical circuit analogy, Γ_{diff}, α and Γ_{sol} can be considered to be conductances for mass transfer.

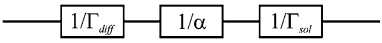

Fig. 2.7 Electrical resistance analogy for non-reactive uptake

An alternative, equivalent kinetic framework for aerosol uptake has been proposed by Pöschl et al. [22]. In this model aerosol particles are considered to have a surface double-layer, consisting of a sorption layer and a quasi-static layer, where the uptake or loss of volatile and non-volatile molecules occurs, respectively. This framework is particularly useful for describing reactive uptake.

Each of the three resistances to uptake will now be examined in more detail.

2.2.1.2 Gas-phase Diffusion

The rate of gas-phase diffusion is straightforward to calculate in the case of uptake by a bulk liquid surface. Diffusion is governed by a continuous concentration gradient of the species being taken up, which is assumed to extend to the interface, as represented the Maxwell equation (1890) [1, 23]:

$$\frac{\partial c_R}{\partial t} = -\frac{1}{R^2}\frac{\partial}{\partial R}(R^2 J_R) \tag{2.16}$$

where c_R is the concentration of the species at a radial position R, t is time and J_R is the molar flux of the species at R. This assumption works well for aerosol droplets which are large compared with the mean free path of the gas-phase molecules, for example in the case of droplets >100 μm in radius at atmospheric pressure [23]. However, for smaller droplets, which are more abundant in the atmosphere, gas diffusion has no straightforward analytical solution [15]. This is because the concentration gradients of gas-phase species within about one mean free path of the surface are considerably altered compared to those far from the droplet [23].

Commonly the empirically-determined Fuchs–Sutugin relation is used to describe the resistance to uptake caused by gas-phase diffusion for a stationary droplet [1, 15, 19]:

$$\frac{1}{\Gamma_{diff}} = \frac{0.75 + 0.283Kn}{Kn(1 + Kn)} \tag{2.17}$$

where Kn is the dimensionless Knudsen number, given by [1, 12]:

$$Kn = \frac{\lambda_{mfp}}{r} \tag{2.18}$$

where λ_{mfp} is the gas-phase molecular mean free path and the r is the droplet radius. The mean free path of a gas-phase molecule in an ideal gas is given by [14]:

$$\lambda_{mfp} = \frac{k_B T}{\sqrt{2}\pi d_g^2 p} \tag{2.19}$$

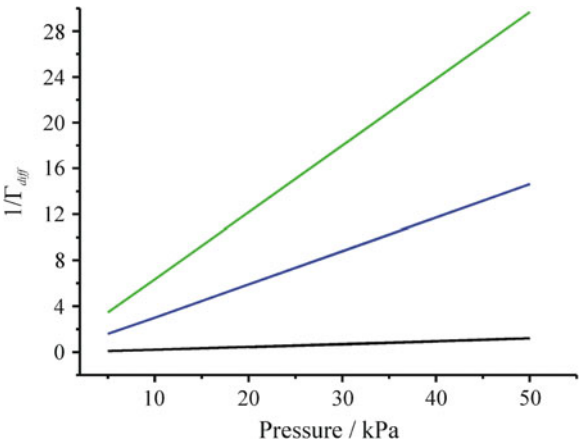

Fig. 2.8 The dependence of $1/\Gamma_{diff}$ on pressure for droplet radii of 0.5, 5 and 10 μm, shown in *black*, *blue* and *green*, respectively

where d_g is the diameter of the gas molecules (m) and p is the pressure (Pa). Hence for uptake of a given molecular species $1/\Gamma_{diff}$ varies with temperature, pressure and the particle size. As the temperature increases or the pressure or particle size decreases, $1/\Gamma_{diff}$ decreases. The dependence of $1/\Gamma_{diff}$ on pressure for the diffusion of water in air of 100% RH for droplet radii of 0.5, 5 and 10 μm is shown in Fig. 2.8.

The mean free path is often expressed in the following equivalent form [15]:

$$\lambda_{mfp} = \frac{3D_g}{\bar{c}} \tag{2.20}$$

where D_g is the diffusion constant of the gas-phase species in the surrounding gas medium ($m^2\ s^{-1}$). D_g depends on the properties of both the diffusing molecules (such as their size and shape) and the medium (such as its viscosity), and the interaction between the two.

The Fuchs–Sutugin relation is valid over a wide range of *Kn* [19]. It assumes a static spherical boundary condition around the droplet [19, 24].

2.2.1.3 Mass Accommodation

The proportion of colliding molecules which will be incorporated into the surface is described by the mass accommodation coefficient, α [9, 12]:

$$\alpha = \frac{\text{number of molecules adsorbed into the bulk}}{\text{number of molecular collisions with the surface}} \tag{2.21}$$

This is effectively a sticking probability and hence takes values from 0 to 1. The value of α depends on the intermolecular interactions between the adsorbing molecule and the surface and can be considered as a surface resistance to uptake.

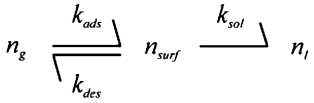

Fig. 2.9 Two-stage mass accommodation process

Mass accommodation is commonly represented as a two-stage process; molecules are first adsorbed at the surface and then transferred to the bulk [25, 26]. Adsorbed species may also desorb from the surface back into the gas phase. This process is illustrated in Fig. 2.9, where k_{ads}, k_{des} and k_{sol} are the rate constants for surface adsorption, surface desorption and solvation, respectively. The rate of re-evaporation is excluded from this description as this effect is dealt with by Γ_{sol}. The number concentrations of the species in the gas-phase, at the surface and in the liquid-phase are represented by n_g, n_{surf} and n_l, respectively.

Molecules can only be considered to be adsorbed if they become thermally equilibrated with the surface; the quantity describing the probability of a molecule equilibrating with the surface is the thermal accommodation coefficient, s. Studies of the uptake of deuterated water on water droplets have shown that D-H isotope exchange on the surface proceeds with unit probability and it can therefore be assumed that $s = 1$ at typical experimental temperatures [18]. Several other studies have also concluded that s is likely to be equal to one under atmospheric conditions [22, 27].

The temperature dependence of α can provide information about the mechanism of uptake at a surface. Using the two-stage model of mass accommodation outlined above and considering α as the proportion of molecules which become thermally accommodated at the surface less the proportion which desorb, a flux balance can be written [12]:

$$\frac{\alpha n_g \bar{c}}{4} = \frac{s n_g \bar{c}}{4} - n_s k_{des} \tag{2.22}$$

This net incoming flux at the surface must be equal to the flux into the liquid [12, 18]:

$$\frac{\alpha n_g \bar{c}}{4} = n_s k_{sol} \tag{2.23}$$

Combining these two equations to eliminate n_g and n_s gives:

$$\frac{\alpha}{s - \alpha} = \frac{k_{sol}}{k_{des}} \tag{2.24}$$

As discussed above s can be taken to be unity and so:

$$\frac{\alpha}{1 - \alpha} = \frac{k_{sol}}{k_{des}} \tag{2.25}$$

Replacing the rate constants, k, using the appropriate expressions for Gibbs free energy of activation, ΔG^* (J mol^{-1}), determined from transition state theory [14]:

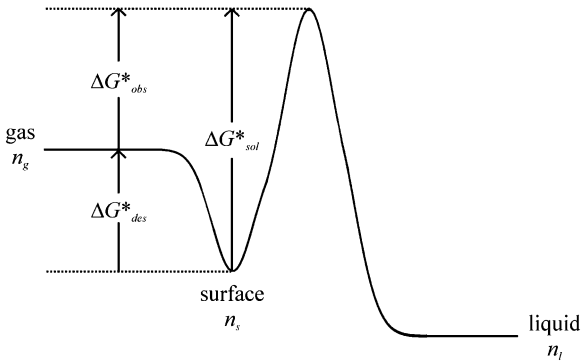

Fig. 2.10 A postulated free energy diagram for the two-stage model of mass accommodation [28]

$$\Delta G^* = -RT \ln \frac{k_B T}{hk} \tag{2.26}$$

where h is Planck's constant (J s), yields [25, 26]:

$$\frac{\alpha}{1-\alpha} = \frac{\exp\left(\frac{-\Delta G^*_{sol}}{RT}\right)}{\exp\left(\frac{-\Delta G^*_{des}}{RT}\right)} = \exp\left(\frac{-\Delta G^*_{obs}}{RT}\right) \tag{2.27}$$

where ΔG^*_{sol} is the free energy of activation for solvation of an absorbed molecule into the bulk, ΔG^*_{des} is the free energy of activation for desorption of a molecule from the surface to the gas phase and hence ΔG^*_{obs} is the free energy of transition for the uptake of a molecule from the gas into the bulk. A free energy diagram postulated by Nathanson et al. to illustrate the two-stage model of mass accommodation is provided in Fig. 2.10 [28].

The temperature dependence of α allows the sign of ΔG^*_{obs} and hence the relative sizes of ΔG^*_{sol} and ΔG^*_{des} to be determined. If ΔG^*_{obs} is negative then a negative temperature dependence of α would be observed.

ΔG^*_{obs} is related to the observed enthalpy and entropy changes of activation by [14]:

$$\Delta G^*_{obs} = \Delta H^*_{obs} - T\Delta S^*_{obs} \tag{2.28}$$

ΔH^*_{obs} and ΔS^*_{obs} were found to be negative for water uptake on a water surface by Li et al. by fitting of Eq. 2.27 to experimental data collected at temperatures varying between 250 and 290 K [18]. They reason that the patterns in the values of ΔH^*_{obs} and ΔS^*_{obs} measured for the uptake of a range of small molecules are consistent with a mechanism of uptake which involves the formation of a loosely-bound trace-gas/water cluster at the gas/liquid interface [18, 28].

There remains debate over the temperature dependence of α, however, [9]. While the study by Li et al. observed a clear dependence on temperature, a study by Winkler et al. observed no temperature dependence over the same temperature range [29]. The experiments from these two studies were, however, conducted under dramatically different conditions, sufficiently so that it has been speculated

that the mechanism for mass accommodation may be different in the two cases [9]. The experimental differences will be discussed later in this chapter.

2.2.1.4 Solubility

$1/\Gamma_{sol}$ describes the resistance to uptake resulting from equilibrium liquid/gas partitioning of the species of interest. This will determine the proportion of molecules entering the bulk which remain and do not re-evaporate. Henry's law relates the partial pressure of a species, p (Pa), to its solution phase concentration, C (mol m^{-3}) [14]:

$$p = HC \tag{2.29}$$

where H is Henry's Law constant (Pa m^3 mol^{-1}). In the case of uptake of a trace species into water droplets during droplet train experiments, Γ_{sol} has been shown to be described by [18]:

$$\frac{1}{\Gamma_{sol}} = \frac{\bar{c}}{8RTH}\sqrt{\frac{\pi t}{D_l}} \tag{2.30}$$

where t is the gas–liquid interaction time (s) and D_l is the liquid-phase diffusion constant of the molecules in water (m^2 s^{-1}). The resistance as a result of liquid/gas-phase partitioning increases with interaction time as a result of the solubility limit of the trace species being approached.

In these studies, however, we are dealing with the uptake of water into an aqueous droplet and in this case it is not clear what value of H would be appropriate. Previous experimental studies have proved inconclusive as to whether resistance due to solubility should be considered in the case of water uptake on water [18]. $1/\Gamma_{sol}$ is therefore neglected in the following analysis.

2.2.2 Consideration of the Rate Determining Step

In the absence of reactions and solubility considerations, the rate of uptake will be limited by gas-phase diffusion and mass accommodation. It is important to understand the relative size of the resistances to uptake arising from these processes in order to determine which, if either, is the rate-controlling process. This is important both in terms of understanding atmospheric processes and for designing experiments to measure mass transfer coefficients.

Three flow regimes exist, characterised by the value of the dimensionless Kn. Which process controls the rate of uptake depends on which flow regime applies. As previously introduced, Kn is the mean free path of gas-phase molecules, λ_{mfp}, divided by a representative physical length scale. Here the droplet radius is the appropriate representative physical length scale. For uptake of a given molecular species, Kn varies with temperature, pressure and the particle size.

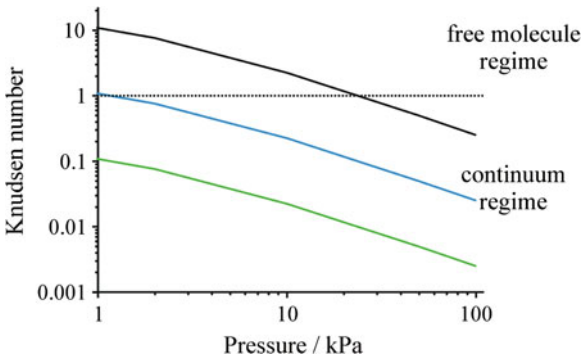

Fig. 2.11 The variation of *Kn* with pressure at a temperature of 291 K for three particle sizes; 0.5 μm (*black line*), 5 μm (*blue line*) and 50 μm (*green line*)

The regimes and the associated *Kn* are [1, 22]

1. The continuum regime: $Kn \ll 1$
2. The transition or Knudsen regime: $Kn \sim 1$
3. The free molecule regime: $Kn \gg 1$

In the continuum regime molecules do not travel far between collisions compared with the size of the particle undergoing uptake. The rate of gas-phase diffusion is slow compared to mass accommodation and uptake can be analysed using gas-phase diffusion equations as this process is limiting. This regime is characteristic of high pressure or low temperature and large particle sizes. In the free molecule regime gas-phase molecules travel a long way between collisions compared with the length scale of the particle, and hence the rate of gas-phase diffusion is not limiting. Mass accommodation at the surface becomes the rate determining process. In the transition regime mass transport can be influenced by both processes. The variation of *Kn* with pressure is shown in Fig. 2.11 at a temperature of 291 K for three particle sizes.

It can be seen from Fig. 2.11 that as the pressure is reduced the regime in which mass accommodation dominates is approached. For small droplets the transition between regimes occurs at higher pressures. For very large droplets gas diffusion can be seen to dominate at all pressures. Mass accommodation is important for uptake by 0.5 μm radius particles at most atmospheric pressures. This size is typical of the atmospheric aerosol accumulation mode, which accounts for most of the aerosol surface area and much of the mass in the atmosphere [1]. This emphasizes the importance of understanding mass accommodation as it is likely to be the rate determining step for a large proportion of atmospheric aerosols.

2.2.3 Atmospheric Importance of α

The rigorous determination of α for water on aqueous surfaces is vitally important for atmospheric science for a number of reasons, including:

- For inclusion in cloud physics models. It is important to consider if the growth of aerosol particles, which may result in them becoming cloud condensation nuclei, is thermodynamically or kinetically determined [30]; α is a key parameter in this process.
- For establishing suitable residence times in experimental chambers, for example cloud condensation chambers [30] and differential mobility analysers [31], kinetic limitations on the rate of droplet growth must be considered.
- For understanding the effect of aerosol composition, and in particular surface composition, on α. Taking into account the presence of surface-active organic compounds in aerosol droplets may result in the growth of particles moving from the equilibrium to the kinetically-controlled regime under certain conditions [30].

Each of these situations will now be discussed in more detail.

2.2.3.1 Cloud Physics Models

The mass accommodation coefficient of water on aqueous surfaces is fundamental to understanding the activation of aerosol particles to act as cloud condensation nuclei (CCN). As discussed in Sect. 2.1.2, the variation of the equilibrium size with RH of a particle consisting of soluble inorganic species can be described by a Köhler plot [1]. Once a particle reaches a certain supersaturated RH, known as the droplet critical supersaturation, S_c, it is termed 'activated' and will grow spontaneously, limited only by the kinetic resistances detailed above [1, 30]. These kinetic limitations, including mass accommodation, must be quantified in order to determine whether the growth of aqueous aerosol droplets as they approach and surpass S_c is thermodynamically or kinetically controlled. If the growth of aerosol particles in the atmosphere is purely thermodynamically controlled then the droplets will always be in equilibrium with the surrounding RH and the size distributions of CCN can be determined from knowledge of the local RH and temperature conditions and equilibrium Köhler theory. If, however, the kinetics of droplet growth play a role then this must be taken into consideration in order to accurately predict the distributions of activated particles. The distribution of activated droplets in turn controls the size and number distributions of cloud droplets, which determine the light scattering properties and stability of clouds and hence have an effect on their radiative forcing, termed the aerosol indirect effect [8, 10, 30, 32–36].

Currently many cloud modelling studies assume aerosol sizes are thermodynamically determined, with the number of activated CCN, n_{CCN}, predicted from the local supersaturation, S [10]:

$$n_{CCN} = AS^B \tag{2.31}$$

where A and B are empirically determined parameters. This assumption may, however, result in an overestimate of the radiative forcing by aerosols, by several

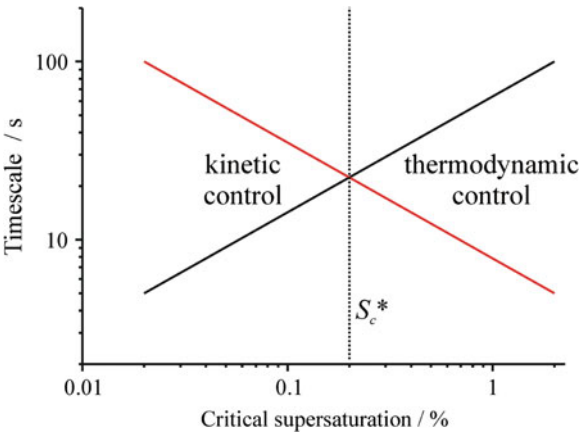

Fig. 2.12 Plot to illustrate the crossover between the regimes of kinetically- and thermodynamically-controlled particle size. τ_{growth} and τ_{eqm} are shown in *red* and *black*, respectively. The quantities on this plot, although typical of atmospheric conditions, are for illustrative purposes only

W m^{-2}, as more particles will be assumed to become activated than if kinetic limitations are taken into account [30, 34].

An alternative view is that neglecting kinetics of droplet growth leads to underestimating the number of activated particles and hence the radiative forcing by the aerosol indirect effect. It is argued that it if growth is delayed by kinetic factors then conditions of higher supersaturation will exist because less water vapour condenses onto droplets, ultimately leading to a greater number of activated particles, resulting in more, but smaller, cloud droplets [9]. This illustrates the level of debate in this area and the importance of furthering the understanding of aerosol uptake processes.

Whether or not kinetics play a role in determining the size of droplets depends on how the timescale of droplet growth, τ_{growth}, compares with the timescale on which the local RH changes, τ_{eqm}. As warm air parcels rise in the atmosphere their temperature decreases, causing the local RH to increase, with the result that the droplets must grow in order to stay in equilibrium. It is useful to define the S_c at which $\tau_{growth} = \tau_{eqm}$, namely S_c^*. Above this value kinetics are unimportant, while below this they must be considered, as illustrated in Fig. 2.12.

S_c^* has been modelled by comparing the timescales for the rate of change of RH in a typical air parcel, using a cloud parcel model, with the timescale for the rate of droplet growth derived from the growth equations of Fukata and Walter [23, 30]. It was found that S_c^* is sensitive to the value of α only for $\alpha < 0.1$ [30]. Hence, if $\alpha > 0.1$ precise knowledge of α is not necessary for determining whether equilibrium or kinetics determine droplet activation. Further to this, cloud modelling studies have found that under typical atmospheric conditions, because of the competing effects of the resistances of mass accommodation and gas-phase diffusion, the proportion of activated droplets is relatively insensitive to changes in α for $\alpha > 0.1$ [18, 23]; hence for these purposes precise knowledge of α is not necessary for evaluating the kinetic factors unless $\alpha < 0.1$. Cloud modelling studies suggest that α cannot be < 0.036 [36, 37].

2.2.3.2 Experimental Equilibration Timescales

It is important to consider the appropriate residence time to use for experimental chambers in the study of CCN size and number distributions. For example, previous studies using cloud condensation chambers [30] and differential mobility analysers [31] have allowed times of seconds to tens of seconds for droplet equilibration. However, calculations including kinetic limitations on the rate of droplet growth and relying on knowledge of α have found that timescales of droplet growth can in fact vary from less than a second up to hundreds of seconds [30], indicating that much longer equilibration times should be used.

If the thermodynamically-determined growth of aerosol particles is examined without accounting for kinetic limitations then underestimated values of droplet growth factors will be reported.

2.2.3.3 Effect of Composition

As well as establishing the value of α for pure water surfaces, it is also important to understand the dependence of α on droplet composition. A technique which is sufficiently sensitive to resolve the variation of α with droplet composition is highly desirable.

It is well established that the presence of organic species can affect the thermodynamic behaviour of inorganic aqueous droplets [38, 39], hence affecting the distribution of particles between the kinetic and equilibrium regimes for a given local supersaturation. The effect of organics on equilibrium droplet behaviour has been studied using optical tweezers by Reid and co-workers [40].

Organic species may also have a dramatic effect on aerosol kinetics via α, although this has not yet been definitively proven [31]. As organic species tend to be hydrophobic in nature there is a tendency for them to partition to the droplet surface, so even small quantities may be effective in retarding mass accommodation at the surface [41]. While some studies have found no effect on the uptake kinetics of water surfaces by an insoluble organic film [28], others have found a clear effect [42, 43]. A study of the rate of water evaporation from liquid microjets revealed an extreme sensitivity of the evaporation coefficient to the composition of the liquid phase [13], which suggests that α may too be highly sensitive to composition. In a study by Tuckermann et al. the relative permittivities of a range of surfactants to water evaporation were measured. This work indicated that the nature of the organic compound is important in determining the mass transport properties of aerosol [36]. This supports suggestions that the kinetics of droplet activation vary with geographical area, depending on the composition of aerosol particles present [13].

An indication that surface-active compounds may have an effect on the mass transfer processes of aerosol droplets has previously been gained using optical tweezers. A step-change in the evaporation rate of a surfactant-containing aqueous droplet was observed, proposed to be associated with formation of a complete

surface coverage of surfactant molecules retarding evaporation of water from the droplet [44]. The same behaviour has been observed for droplets containing atmospheric organics isolated using an electrodynamic balance [45] and the technique of acoustic levitation [36].

2.2.4 Importance in Other Fields

The relevance of the work described in this thesis is not limited to atmospheric science. Many industrial processes depend on mass transfer to and from aerosol particles, for example the burning of fuel in combustion engines. In addition, in the practice of drug delivery to the lungs using medical nebulisers it is important to understand the relative timescale of the passage of the drugs through the airways during inhalation compared with that of water uptake as a result of increasing RH inside the body. This is necessary in order to determine the size of the drug-containing particles when they reach the surfaces of the lungs in order to evaluate their penetration efficiency to the bloodstream.

2.2.5 Evaporation from an Aerosol Droplet

The equivalent model for evaporation of water molecules from an aqueous droplet involves reversible transport of liquid-phase molecules to and from the surface, followed by desorption from the surface to the gas phase and gas-phase diffusion away from the droplet. The maximum rate of evaporation is hence limited by gas-phase diffusion and a resistance associated with the surface.

The maximum evaporative flux, $J_{e,max}$, is again given by the Hertz–Knudsen equation [13]:

$$J_{e,\max} = \frac{\Delta p_{w,d}}{\sqrt{2\pi M_e k_B T}} \tag{2.32}$$

where M_e is the relative molecular mass of the evaporating species (kg).

The overall resistance to evaporation is described by a constant, $\gamma_{e,meas}$, which includes the effects of gas-phase diffusion and the surface resistance. The measured evaporative flux, $J_{e,meas}$, is given by [13]:

$$J_{e,meas} = \gamma_{e,meas} J_{e,\max} \tag{2.33}$$

The surface resistance is associated with both the reversible transport of liquid-phase molecules to and from the surface and desorption from the surface to the gas phase. The appropriate surface conductance for this process is the evaporation coefficient, γ_e. Analogous to the resistance model for uptake, the overall resistance to evaporation can be described by

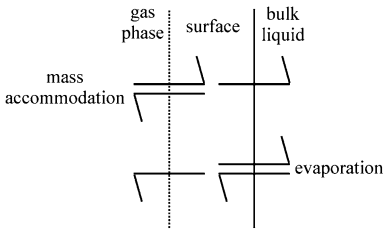

Fig. 2.13 Surface processes associated with mass accommodation and evaporation

$$\frac{1}{\gamma_{e,meas}} = \frac{1}{\Gamma_{diff}} + \frac{1}{\gamma_e} \tag{2.34}$$

Knudsen defined γ_e as [46]:

$$\gamma_e = \frac{\text{number of molecules transferred to the vapour phase}}{\text{number of molecules emitted from the liquid phase}} \tag{2.35}$$

This describes the proportion of molecules which arrive at the interface from the bulk and which eventually desorb from the surface. As for α, γ_e can take values between 0 and 1.

There is disagreement in the published literature over whether α and γ_e are physically equivalent quantities and should therefore have the same value. It has been argued that by microscopic reversibility they are equivalent quantities [12]. Several studies claim equivalence of the two values and quantify α via purely evaporative measurements [30, 47]. Other authors reason that although the processes are closely related they are not physically equivalent and hence there is no reason why the values should be the same [13, 46].

Whether the quantities are equivalent depends on the formulations for uptake and evaporation used. Figure 2.13 illustrates that in the formulation used in this work the processes associated with the resistances described by $1/\alpha$ and $1/\gamma_e$ are not physically equivalent.

The experimental approach used in this work represents a valuable opportunity to study both evaporation and uptake under identical experimental conditions. Both quantities will be determined without the need for any prior assumption about their equivalence.

Knowledge of γ_e is important for atmospheric studies. While γ_e it is not involved in determining particle number concentrations, it is involved in determining droplet size distributions, which are important for quantifying the aerosol direct effect.

2.2.6 Previous Experimental Studies

Despite the significance of aerosol mass transport, α and γ_e remain highly contentious quantities. Over forty experimental studies of α have been published since

the first measurement by Rideal in 1925 [9, 31]. The reported values of α span three orders of magnitude, from $\sim$0.001 to 1 [9]. Reported values of γ_e also span three orders of magnitude [13].

Measurement of aerosol mass transport is challenging; it was even claimed in 1975 by Sherwood et al. that "not only is there no useful theory to employ in predicting α, there is no easy way to experimentally measure it." [17, 48]. Determination of α or γ_e generally relies on measuring a rate of mass transfer and comparing this with the theoretical rate. As a result, determination is not straightforward because the magnitude of the other resistances to mass transport must be well-known. In particular the resistance from gas-phase diffusion is problematic. Under standard experimental conditions this factor will tend to dominate the determination of the rate of mass transfer and as a consequence α and γ_e can be difficult to elucidate. Conditions of low pressure will often be needed to address this and increase the sensitivity of experiments. There are problems associated with how to deal with gas-phase diffusion, because, as outlined above, no analytical solution exists in the case of small particles. Knowledge of surface temperature and the maintenance of a surface free from contaminants are other experimental challenges.

Previous experimental studies of α and γ_e for water at an aqueous surface can be separated into three broad categories, based on the form of the surface being investigated:

- Bulk, planar sample of liquid phase
- Ensemble of droplets
- Single droplet

For a given technique the rate of mass transfer may be measured in a variety of ways:

- Change in volume of the liquid phase
- Change in liquid-phase composition
- Change in gas-phase composition

The latter two measurement techniques rely on isotopic labelling, for example using $H_2^{17}O$ or D_2O as the gas-phase species undergoing uptake [18].

2.2.6.1 Bulk Techniques

Bulk sample techniques are used to investigate the rate of uptake by a macroscopically flat surface. One example of a bulk technique employs a vertical or horizontal wetted wall flow reactor, for which uptake into a liquid flowing on the inner surface of a tube is measured. Rideal's early measurement was a bulk technique which measured the transfer of water between two chambers held at different temperatures and connected by a tube [31]. Uptake in this type of system takes place in the continuum regime and hence the effect of gas-phase diffusion is easier to interpret than in the case of studies on particles in the free particle or

transition regime, although dominance of gas-phase diffusion limits the sensitivity of such techniques to surface accommodation. These techniques offer little insight into the uptake of atmospheric aerosol particles for which surface accommodation is often more important than gas-phase diffusion.

2.2.6.2 Ensembles of Droplets

Measurements on ensembles of droplets have recently been carried out by two groups; a collaboration between the Universities of Vienna and Helsinki (UV/UH) [29, 49] and another between Boston College and Aerodyne Research Inc. (BC/ARI) [18]. The former study reports that $\alpha = 1$ while the later reports values of 0.17 ± 0.03 at 280 K and 0.32 ± 0.04 at 258 K.

The BC/ARI studies were performed using a droplet train flow reactor [15, 50–53]. The droplets are created by a vibrating orifice aerosol generator (VOAG) with a backing pressure and then fall through a gas in a sealed flow tube. Successive droplets are generally separated by several droplet diameters. The change in the gas-phase composition is monitored using infrared absorption spectroscopy and used to derive the amount of uptake taking place. The change in gas-phase concentration of $H_2^{17}O$ as a function of available droplet surface area for uptake is used to determine α for water self-accommodation. Experiments were also carried out for uptake of D_2O. This case represents reactive uptake, because of rapid isotopic substitution of H and D atoms, and a higher rate of uptake is observed, as expected.

Measurements were carried out at a range of pressures and hence *Kn*; measurements were performed for $0.04 \leq Kn \leq 0.6$. This technique offers a continually-renewed liquid-phase surface which prevents the build-up of contaminants. The VOAG produces droplets of a well defined size so the surface area for uptake is well known; this is a crucial quantity for analysis of the experimental data.

In the analytical procedure for this work, gas-phase diffusion is treated using a modified version of the Fuchs–Sutugin relation. Instead of using *Kn*, a modified value of *Kn* is used in which the droplet radius is replaced by an effective radius of twice the orifice radius. This modification of the Fuchs–Sutugin relation has been found to be necessary for fitting the variation of the measured rates of uptake with pressure in this and previous studies from the collaboration [15, 50–52, 54]

This empirical scaling affects the value of $1/\Gamma_{diff}$ and hence the value of α determined by this technique. Although it can be reasoned that no dependence on droplet diameter is expected, this reasoning does not correctly predict the magnitude of the scaling found to be necessary [54]. The reasoning involves considering that the effective droplet surface area for gas-phase diffusion is reduced by a factor of the droplet diameter divided by the distance between droplets, as this is the fraction of the total time that a given region is occupied by a droplet from the train, and that the distance between droplets is a function of droplet diameter and the orifice diameter.

It is not expected that an unmodified Fuchs–Sutugin approach should be appropriate for the analysis of data collected in this way. The Fuchs–Sutugin

relation is based on static boundary conditions not valid for a droplet train experiment [24]. The key consideration is whether diffusive transport to a moving droplet is similar enough to that to a static droplet for a simple modification such as the one used to be valid.

Fluid-dynamical numerical modelling of the flow patterns of falling droplet trains shows that perturbations of diffusive flow to the droplets will exist near droplets, with depletion in the region near to droplet, resulting from microconvection between the droplets caused by their relative flow [19, 24]. This would result in an increase in the gas-phase resistance to uptake. This modelling work found that an effective radius of 1.2 times the droplet radius should be required to account for this additional gas-phase resistance in the case of falling droplets, which is considerably larger than twice the orifice radius [19]. A further fluid dynamical simulation showed that even with modification, the Fuchs–Sutugin relation cannot exactly represent diffusion to a train of moving droplets [55]. Because of the uncertainty surrounding treating diffusion to moving droplets, this fluid dynamical study suggests that the results of the BC/ARI study are consistent with a value of α of between 0.2 and 1.

The UV/UH experiment involves monitoring the rate of growth of water droplets using Mie scattering as they grow in an expansion chamber. The droplets are formed by condensation onto silver particles and then introduced into an expansion chamber, where they experience saturation ratios of 1.3–1.5. Gas-phase diffusion is accounted for and the observed growth curves are compared to theoretical curves in order to determine α. The study excluded values of $\alpha < 0.80$ for temperatures of 250–270 K and values of $\alpha < 0.4$ for temperatures up to 290 K. They conclude that all of their data are consistent with a value of $\alpha = 1$.

It has been reasoned that the discrepancies in the magnitude and temperature dependence of α between the two studies could be a result of the operation of different mechanisms of mass accommodation [9]. The experimental conditions are certainly considerably different; in the BC/ARI study saturation ratios of 1.01 are typical, while the UV/UH study features ratios of 1.3–1.5. Conditions of saturation as high as 1.3–1.5 are not representative of typical atmospheric cloud formation conditions.

Work by Cappa et al. on evaporation from liquid water microjets under condition of free molecular evaporation showed that the H_2O/D_2O isotope fractionation of evaporating molecules differs from that for vapour at equilibrium and that the fractionation depended on the D_2O mole fraction and temperature [13]. They reasoned that this indicates that there is an energetic barrier to evaporation and hence γ_e and α must be less than one.

2.2.6.3 Single Droplet Studies

A recent study by Zientara et al. used single droplets isolated using an electrodynamic balance [30]. The evolution of the size of evaporating droplets was investigated using elastic light scattering and compared with theory in order to

determine γ_e. γ_e is considered equivalent to α and results were obtained in good agreement with the magnitude and dependence of those of the BC/ARI collaboration; $\alpha \sim 0.18$ at 273.1 K and ~ 0.13 at 293.1 K.

Shaw and Lamb used an electrodynamic balance to simultaneously measure the rate of homogeneous nucleation of ice and the evaporation rate of liquid water droplets as a function of pressure [47]. The homogeneous nucleation rate is used as a highly sensitive measure of droplet temperature, and as the temperature of an evaporating droplet is a function of γ_e and the thermal accommodation coefficient, these quantities are determined. They assumed that γ_e and α are equal and reported $0.04 < \alpha < 0.1$ at a temperature of 238.1 K.

2.2.7 Field Studies

The mass accommodation coefficient has been investigated in field studies. The studies, termed CCN closure experiments, compare observations of CCN concentration with concentrations predicted for given particle size and composition distributions [56]. When closure is not achieved it is usually the case that the CCN concentration has been over predicted. Assuming that the discrepancy can be attributed to kinetic limitations on droplet activation a value of α can be determined. One such study found that closure was achieved by using a value of α of 0.06, although it was found that the value can vary from 0.03 to 1.0 [57]. Similar studies have shown that the value of α necessary to correctly predict the CCN concentration varies considerably from day to day and even during the same day, attributed to chemical aging of the aerosol particles [56]. These studies highlight the importance of resolving the effects of aerosol composition on mass transfer.

2.2.8 Theoretical Work

Several molecular dynamics (MD) studies have reported a water self-accommodation coefficient of close to or equal to unity for temperatures between 300 and 350 K [55, 58, 59]. A study has also suggested that α is the same regardless of the molecule being taken up [58]. The MD studies do not agree with experiments which find that α is < 1, that it is temperature dependent and that interactions between the gas-phase species and the surface are important.

Davidovits et al. have questioned whether MD simulations can adequately simulate uptake on a water surface [60]. It has been suggested that the restricted spatial and temporal scales of MD simulations mean that these studies sample a different accommodation process to that studied in laboratory experiments [9].

It is also thought that the potential energy surfaces used in the simulations do not adequately describe the real situation.

2.2.9 Summary

This chapter has outlined the factors which determine the equilibrium droplet size. These factors form the basis of the technique for measuring droplet absorption described in Chap. 6. The theoretical framework for understanding the kinetics of aerosol mass transfer has also been described, as well as the atmospheric significance of the mass accommodation coefficient of water at an aerosol surface. Studies of the kinetics of aerosol mass transfer are the subject of Chap. 7.

References

1. J.H. Seinfeld, S.N. Pandis, *Atmospheric Chemistry and Physics: From Air Pollution to Climate Change* (Wiley, New York, 1998)
2. C. Pilinis, S.N. Pandis, J.H. Seinfeld, J. Geophys. Res. Atmos. **100**, 18739 (1995)
3. S.L. Clegg, P. Brimblecombe, A.S. Wexler, J. Phys. Chem. A **102**, 2155 (1998)
4. I.N. Tang, H.R. Munkelwitz, Atmos. Environ. Part A–General Topics **27**, 467 (1993)
5. A.J. Prenni, P.J. De Mott, S.M. Kreidenweis, Atmos. Environ. **37**, 4243 (2003)
6. H. Köhler, Geofysiske Publikasjoner **2**, 3 (1921)
7. G.B. Ellison, A.F. Tuck, V. Vaida, J. Geophys. Res. Atmos. **104**, 11633 (1999)
8. D. Rosenfeld, Science **287**, 1793 (2000)
9. P. Davidovits et al., Geophys. Res. Lett. **31**, L22111 (2004)
10. R.J. Charlson, S.E. Schwartz, J.M. Hales, R.D. Cess, J.A. Coakley, J.E. Hansen, D.J. Hofmann, Science **255**, 423 (1992)
11. R.J. Charlson, S.E. Schwartz, J.M. Hales, R.D. Cess, J.A. Coakley, J.E. Hansen, D.J. Hofmann, Science **256**, 598 (1992)
12. P. Davidovits, C.E. Kolb, L.R. Williams, J.T. Jayne, D.R. Worsnop, Chem. Rev. **106**, 1323 (2006)
13. C.D. Cappa, W.S. Drisdell, J.D. Smith, R.J. Saykally, R.C. Cohen, J. Phys. Chem. B **109**, 24391 (2005)
14. P. Atkins, J. de Paula, *Physical Chemistry* (Oxford University Press, Oxford, 2002)
15. Q. Shi, Y.Q. Li, P. Davidovits, J.T. Jayne, D.R. Worsnop, M. Mozurkewich, C.E. Kolb, J. Phys. Chem. B **103**, 2417 (1999)
16. S.E. Schwartz, J.E. Freiberg, Atmos. Environ. **15**, 1129 (1981)
17. S.E. Schwartz, in *Chemistry of Multiphase Atmospheric Systems* ed. by W. Jaeschke (Springer, Heidelberg, 1986), p. 415
18. Y.Q. Li, P. Davidovits, Q. Shi, J.T. Jayne, C.E. Kolb, D.R. Worsnop, J. Phys. Chem. A **105**, 10627 (2001)
19. M. Sugiyama, S. Koda, A. Morita, Chem. Phys. Lett. **362**, 56 (2002)
20. D.R. Hanson, A.R. Ravishankara, J. Phys. Chem. **97**, 12309 (1993)
21. D.R. Hanson, A.R. Ravishankara, E.R. Lovejoy, J. Geophys. Res. Atmos. **101**, 9063 (1996)
22. U. Pöschl, Y. Rudich, M. Ammann, Atmos. Chem. Phys. **7**, 5989 (2007)
23. N. Fukuta, L.A. Walter, J. Atmos. Sci. **27**, 1160 (1970)

24. J.F. Widmann, E.J. Davis, J. Aerosol Sci. **28**, 1233 (1997)
25. J.T. Jayne, S.X. Duan, P. Davidovits, D.R. Worsnop, M.S. Zahniser, C.E. Kolb, J. Phys. Chem. **95**, 6329 (1991)
26. P. Davidovits, J.T. Jayne, S.X. Duan, D.R. Worsnop, M.S. Zahniser, C.E. Kolb, J. Phys. Chem. **95**, 6337 (1991)
27. M. Zientara, D. Jakubczyk, K. Kolwas, M. Kolwas, J. Phys. Chem. A, **112**, 5152 (2008)
28. G.M. Nathanson, P. Davidovits, D.R. Worsnop, C.E. Kolb, J. Phys. Chem. **100**, 13007 (1996)
29. P.M. Winkler, A. Vrtala, P.E. Wagner, M. Kulmala, K.E.J. Lehtinen, T. Vesala, Phys. Rev. Lett. **93**, 075701 (2004)
30. P.Y. Chuang, R.J. Charlson, J.H. Seinfeld, Nature **390**, 594 (1997)
31. M.N. Chan, C.K. Chan, Atmos. Chem. Phys. **5**, 2703 (2005)
32. IPCC, Climate Change 2007: The Physical Science Basis. Contribution of Working Group I to the Fourth Assessment Report of the Intergovernmental Panel on Climate Change, ed. by S. Solomon, D. Qin, M. Manning, Z. Chen, M. Marquis, K.B. Averyt, M. Tignor, H.L. Miller (Cambridge University Press, Cambridge, New York, USA, 2007)
33. IPCC, Climate Change 2001: The Physical Science Basis. Contribution of Working Group I to the Third Assessment Report of the Intergovernmental Panel on Climate Change, ed. by F. Joos, A. Ramirez-Rojas, J.M.R. Stone, J. Zillman (Cambridge University Press, Cambridge, New York, USA, 2001)
34. A. Nenes, S. Ghan, H. Abdul-Razzak, P.Y. Chuang, J.H. Seinfeld, Tellus Series B-Chem. Phys. Meteorol. **53**, 133 (2001)
35. J.G. Hudson, S.S. Yum, J. Atmos. Sci. **54**, 2642 (1997)
36. S.S. Yum, J.G. Hudson, Y.H. Xie, J. Geophys. Res. Atmos. **103**, 16625 (1998)
37. J.G. Hudson, T.J. Garrett, P.V. Hobbs, S.R. Strader, Y.H. Xie, S.S. Yum, J. Atmos. Sci. **57**, 2696 (2000)
38. C.N. Cruz, S.N. Pandis, J. Geophys. Res. Atmos. **103**, 13111 (1998)
39. M.L. Shulman, M.C. Jacobson, R.J. Charlson, R.E. Synovec, T.E. Young, Geophys. Res. Lett. **23**, 603 (1996)
40. K.L. Hanford, L. Mitchem, J.P. Reid, S.L. Clegg, D.O. Topping, G.B. McFiggans, J. Phys. Chem. A **112**, 9413 (2008)
41. G.T. Barnes, Nature **220**, 1025 (1968)
42. E.K. Rideal, J. Phys. Chem. **29**, 1585 (1925)
43. R. Tuckermann, S. Bauerecker, H.K. Cammenga, J. Colloid Interf. Sci. **310**, 559 (2007)
44. J. Buajarern, Ph.D. thesis: Fundamental studies of inorganic and organic aqueous aerosols using optical tweezers, University of Bristol, Bristol, UK, 2007
45. M.L. Shulman, R.J. Charlson, E.J. Davis, J. Aerosol Sci. **28**, 737 (1997)
46. R. Marek, J. Straub, Int. J. Heat Mass Transf. **44**, 39 (2001)
47. R.A. Shaw, D. Lamb, J. Chem. Phys. **111**, 10659 (1999)
48. T.K. Sherwoood, R.L. Pigford, C.R. Wilke, *Mass Transfer* (McGraw-Hill, New York, 1975)
49. P.M. Winkler, A. Vrtala, R. Rudolf, P.E. Wagner, I. Riipinen, T. Vesala, K.E.J. Lehtinen, Y. Viisanen, M. Kulmala, J. Geophys. Res. Atmos.**111**, D19202 (2006)
50. D.R. Worsnop, M.S. Zahniser, C.E. Kolb, J.A. Gardner, L.R. Watson, J.M. Vandoren, J.T. Jayne, P. Davidovits, J. Phys. Chem. **93**, 1159 (1989)
51. E. Swartz, Q. Shi, P. Davidovits, J.T. Jayne, D.R. Worsnop, C.E. Kolb, J. Phys. Chem. A **103**, 8824 (1999)
52. Q. Shi, P. Davidovits, J.T. Jayne, D.R. Worsnop, C.E. Kolb, J. Phys. Chem. A **103**, 8812 (1999)
53. G.N. Robinson, D.R. Worsnop, J.T. Jayne, C.E. Kolb, P. Davidovits, J. Geophys. Res. Atmos.**102**, 3583 (1997)
54. D.R. Worsnop, Q. Shi, J.T. Jayne, C.E. Kolb, E. Swartz, P. Davidovits, J. Aerosol Sci. **32**, 877 (2001)
55. A. Morita, M. Sugiyama, H. Kameda, S. Koda, D.R. Hanson, J. Phys. Chem. B **108**, 9111 (2004)
56. C.R. Ruehl, P.Y. Chuang, A. Nenes, Atmos. Chem. Phys. **8**, 1043 (2008)

57. C. Fountoukis et al., J. Geophys. Res. Atmos.**112**, D10S30 (2007)
58. J. Vieceli, M. Roeselova, D.J. Tobias, Chem. Phys. Lett. **393**, 249 (2004)
59. T. Tsuruta, G. Nagayama, J. Phys. Chem. B **108**, 1736 (2004)
60. P. Davidovits, D.R. Worsnop, L.R. Williams, C.E. Kolb, M. Gershenzon, J. Phys. Chem. B **109**, 14742 (2005)

http://www.springer.com/978-3-642-16347-0

Light-Induced Processes in Optically-Tweezed Aerosol Droplets

Knox, K.J.

2011, XII, 204 p., Hardcover
ISBN: 978-3-642-16347-0